Looseness Detection Utilizing FBG Based Operational Modal Strain for a Bolted Cantilever Plate

Mingyao Liu
School of Mechanical and Electronic Engineering
Wuhan University of Technology
Wuhan, China
myliu@whut.edu.cn

Zechao Wang*
School of Mechanical and Electronic Engineering
Wuhan University of Technology
Wuhan, China
whutwzc@whut.edu.cn

Yongzhi Qu
School of Mechanical and Electronic Engineering
Wuhan University of Technology
Wuhan, China
quwong@whut.edu.cn

Liang Wan
School of Mechanical and Electronic Engineering
Wuhan University of Technology
Wuhan, China
243344151@qq.com

Liu Hong
School of Mechanical and Electronic Engineering
Wuhan University of Technology
Wuhan, China
hongliu@whut.edu.cn

***Abstract*—The cantilever plate structure is widely used in wind tunnel nozzle segments. During the operation of the wind tunnel, the flexible steel plate will bear various complex loads such as shearing, bending and twisting, etc. The bolts of the plate are prone to loosen due to the fatigue damage. The methods based on the electromechanical impedance, sub-harmonic resonance and vision have been presented in the literature. However, the mentioned methods cannot detect the bolt looseness effectively in a harsh environment. To address this issue, we presented a novel method to detect the bolt looseness for the cascaded structures based on the operational strain estimated from Fiber Bragg Grating (FBG). In this work, an improved method of the operational modal analysis (OMA) presented in our previous work is employed. And then an enhanced Structural Damage Indicator (SDI) based on the operational strain is presented to detect and locate the loose bolts. Both the results from experiments and simulations showed that the SDI can detect and locate the loose bolts accurately.**

Keywords-loose bolt; strain mode; fiber Bragg grating; structural damage index

I. INTRODUCTION

The cantilever thin plate structure is a typical structural form in the design of a wind tunnel flexible plate and is widely used in wind tunnel nozzle segments. During the operation of the wind tunnel, the flexible plate needs to bear a variety of complex loads such as shearing, bending and twisting, etc. The bolts are prone to loosen due to its fatigue damage [1]. The looseness of the bolts may further result in the failure of the flexible plate to form the corresponding profile and greatly reduce the flow field properties in the wind tunnel. More seriously, it will cause significant damage to the entire wind tunnel structure and personnel. Therefore, it is of significance to find an effective way to discover the looseness of the bolts in the wind tunnel.

Common methods to detect the loose bolts are based on vibration characteristics [2-4], ultrasonic [5] and electromechanical impedance [6]. Zhou et al. proposed a method to detect the loose bolts based on empirical mode decomposition. However, this method needed to be carried out under harmonic excitation [2]. Based on the work of Zhou et al, Zhang et al. proposed a method for detecting loose bolt based on subharmonic resonance while the method was difficult to accurately locate the loose bolts [3]. Gou et al used the natural frequency method to detect and quantify the pre-tightening force of the bolt. Similarly, this method was difficult to locate the multi-bolt connection structure [4]. Jhang et al. measured the axial force of the bolt based on the ultrasonic method. However, the ultrasonic method was difficult to monitor the bolt in real time under harsh environments [5]. Recently, Jiang et al. used the piezoelectric ceramic as sensors to monitor the bolts looseness [7]. Xu et al. detected the joints of bolts based on the electromechanical impedance method [8]. The method also bears the drawbacks of traditional electrical sensors such as electromagnetic interference. Therefore, the present paper aims to put forward a new method to detect the bolts looseness with advanced sensing technology.

The method based on the natural frequency mentioned above is a global method which is hard to locate the loose bolts. Since

The research is financially supported by the National Natural Science Foundation of China (NSFC), Grant no.51505353

978-1-7281-0860-5/19/$31.00 ©2019 IEEE

the mode shape provided spatial information about the structure, it and can be used to locate the damage. According to the theory of material mechanics, the strain distribution near the damaged area will change abruptly. Therefore, the strain mode shape has more advantages in identifying and locating the loose bolt than the displacement mode shape. Yam et al. have proved that strain mode is more sensitive to local damage than displacement mode [6]. Jiang et al. replaced the traditional strain gauges with FBG sensors for strain modal analysis and damage identification [7]. Subsequently, Xu et al. used FBG sensors to detect and locate the loose bolt of the reinforcing rib excited with an electromagnetic vibration exciter under the natural frequency [8]. However, the structure is unlikely to be in a resonant state during the actual operation. Herein, we put forward a new way to discover the bolts looseness based on the operational strain, which can be applied to the occasion of wind load which cannot be measured.

For the OMA methods, common methods include stochastic subspace identification method, frequency domain decomposition method, least squares complex frequency domain method and Poly-max method. The stochastic subspace identification method is a modal parameter identification method in the time domain. The frequency domain decomposition method was developed in the traditional peak picking method and successfully applied in many engineering fields. The biggest advantage of the least squares complex frequency domain method is the construction of a very clear stabilization graph. The Polymax method is an improved least squares complex frequency domain method by introducing multiple references. However, all the output points needed to be fitted to calculate the mode shape, which increases the computation burden. Therefore, an improved diagram of the Operation Strain Modal Analysis (OSMA) is employed to calculate the modal strain, which is proposed in our previous study [9]. And then an enhanced SDI is presented based on the work of Cui et al. [10] to detect the bolts looseness. The homologous experiments and simulations have been further executed to verify the presented method to detect and locate the loose bolts.

The rest of the paper is composed as follows: Sec. II gives the principle of the measurement; the scenarios of the simulations and experiments are given in Sec. III; and the results and discussions are given in Sec. IV.

II. PRINCIPLE OF MEASUREMENT

A. Operational modal parameter identification

The i^{th} output of the structure denotes to $\varepsilon_i(n)$ and the l^{th} input of the structure is defined as $f_l(n)$. In a linear time-invariant system, the output $\varepsilon_i(n)$ and the input $f_l(n)$ are defined as the generalized stationary random processes. That is to say, the correlation function and average between them remain stable at any time.

Similar to the displacement modal analysis [10], the strain frequency response function can be shown as follows:

$$H_{il}^{\varepsilon} = \sum_{r=1}^{M} \frac{\psi_{ir}^{\varepsilon} \varphi_{ir}}{k_r - \omega^2 m_r + j\omega \cdot c_r} (i = 1,2,\cdots,N_o; l = 1,2,\cdots N_i) \quad (1)$$

where ψ_{ir}^{ε} is the r[th] order strain mode shapes (SMS) of the i[th] output, φ_{ir} is the r[th] order displacement mode shapes (DMS) on l[th] output. k_r denotes the r[th] order modal stiffness. m_r denotes the r[th] order modal mass and c_r denotes the r[th] order modal damping ratio. The (1) can be further decomposed as follows:

$$H_{il}^{\varepsilon}(j\omega) = \sum_{r=1}^{M} \left[\frac{\psi_{ir}^{\varepsilon} \cdot L_{lr}^{T}}{j\omega - \lambda_r} + \frac{\psi_{ir}^{\varepsilon *} \cdot L_{lr}^{H}}{j\omega - \lambda_r^*} \right] \quad (2)$$

where L_r^T is the r[th] modal participation of the l^{th} input, the superscript * is the complex conjugate operator, superscript H is the complex conjugate transpose operator, and λ_r are the r[th] physical poles which can be showed as follows:

$$\lambda_r, \lambda_r^* = -\xi_r \cdot \omega_r \pm j \cdot \sqrt{1 - \xi_r^2} \cdot \omega_r \quad (3)$$

In terms of the OSMA, only the information of the output spectra is available. And the output spectra $\left[S_{yy}^{\varepsilon}(\omega)\right]$ can be expressed as follows:

$$\left[S_{yy}^{\varepsilon}(\omega)\right] = [\mathrm{H}^{\varepsilon}(\omega)] \cdot [S_{II}(\omega)] \cdot [\mathrm{H}^{\varepsilon}(\omega)]^{H} \quad (4)$$

where $[S_{II}(\omega)]$ denotes the input power spectra. Assuming that the $[S_{II}(\omega)]$ is the white noise, we can calculate the output spectrum according to [11]. The formula is given as follows:

$$\left[S_{yy}^{\varepsilon}(j\omega)\right] = \sum_{r=1}^{M} \frac{\{\psi_r^{\varepsilon}\}\langle g_r\rangle}{j\omega - \lambda_r} + \frac{\{\psi_r^{\varepsilon^*}\}\langle g_r^*\rangle}{j\omega - \lambda_r^*} + \frac{\{g_r\}\langle\psi_r^{\varepsilon}\rangle}{-j\omega - \lambda_r} + \frac{\{g_r^*\}\langle\psi_r^{\varepsilon^*}\rangle}{-j\omega - \lambda_r^*} \quad (5)$$

where $\langle g_r \rangle$ is the operational reference factors. The pre-processing technique is required to convert the operational data. Commonly used spectral estimation methods are the modified Welch's period-gram and the weighted correlogram. Herein, the Welch's method is adopted and its advantages are concluded as follows:

1) It is enough to calculate the Positive Strain Power Spectra (PSPS) by utilizing positive correlations.

2) Lower order models can be fitted without influencing quality.

3) The modal decomposition of the PSPS can be obtained as follows:

$$S_{yy}^{\varepsilon}(j\omega)^{+} = \sum_{r=1}^{M} \frac{\{\psi_r^{\varepsilon}\}\langle g_r\rangle}{j\omega - \lambda_r} + \frac{\{\psi_r^{\varepsilon^*}\}\langle g_r^*\rangle}{j\omega - \lambda_r^*} \quad (6)$$

In our previous work [9], the Forsythe complex orthogonal polynomials and the Least squares technique are used to fit the elements of the (6). The method is different from the Polymax because only one element of the Matrix $\left[S_{yy}^{\varepsilon}(j\omega)^{+}\right]$ is used. After obtaining the physical poles, the strain response transmissibility (SRT) will converge to the ratio of the SMS when jω goes to the r[th] system pole λ_r. The derivation is shown as follows:

$$\lim_{j\omega\to\lambda_r} T_{ij}^{\varepsilon}(\omega) = \lim_{j\omega\to\lambda_r} \frac{X_{\varepsilon,i}(\omega)}{X_{\varepsilon,j}(\omega)} = \frac{\psi_{ir}^{\varepsilon}\cdot g_{1r}^{T}\cdot F_1(\omega)+\psi_{ir}^{\varepsilon}\cdot g_{2r}^{T}\cdot F_2(\omega)+\cdots+\psi_{ir}^{\varepsilon}\cdot g_{Nir}^{T}\cdot F_{Ni}(\omega)}{\psi_{jr}^{\varepsilon}\cdot g_{1r}^{T}\cdot F_1(\omega)+\psi_{jr}^{\varepsilon}\cdot g_{2r}^{T}\cdot F_2(\omega)+\cdots+\psi_{jr}^{\varepsilon}\cdot g_{Nir}^{T}\cdot F_{Ni}(\omega)}$$
$$= \frac{\psi_{ir}^{\varepsilon}\cdot[g_{1r}^{T}\cdot F_1(\omega)+g_{2r}^{T}\cdot F_2(\omega)+\cdots+g_{Nir}^{T}\cdot F_{Ni}(\omega)]}{\psi_{jr}^{\varepsilon}\cdot[g_{1r}^{T}\cdot F_1(\omega)+g_{2r}^{T}\cdot F_2(\omega)+\cdots+g_{Nir}^{T}\cdot F_{Ni}(\omega)]} = \frac{\psi_{ir}^{\varepsilon}}{\psi_{jr}^{\varepsilon}} \tag{7}$$

where $X_{\varepsilon,i}(\omega)$ spectra of the ith output and $X_{\varepsilon,j}(\omega)$ is the spectra of the j[th] output. Ground on the (7), the equation can be obtained as follows:

$$\lim_{j\omega\to\lambda_r}\left[T_{1j}^{\varepsilon}, T_{2j}^{\varepsilon}, \cdots, T_{(j-1)j}^{\varepsilon}, 1, T_{(j+1)j}^{\varepsilon}, \cdots T_{Noj}^{\varepsilon}\right] = \left[\frac{\psi_{1r}^{\varepsilon}}{\psi_{jr}^{\varepsilon}}, \frac{\psi_{2r}^{\varepsilon}}{\psi_{jr}^{\varepsilon}}, \cdots, \frac{\psi_{(j-1)r}^{\varepsilon}}{\psi_{jr}^{\varepsilon}}, 1, \frac{\psi_{(j+1)r}^{\varepsilon}}{\psi_{jr}^{\varepsilon}}, \cdots \frac{\psi_{Nor}^{\varepsilon}}{\psi_{jr}^{\varepsilon}}\right] \tag{8}$$

The diagram for the presented diagram of the OMA in our previous study [9] is shown in Fig. 1.

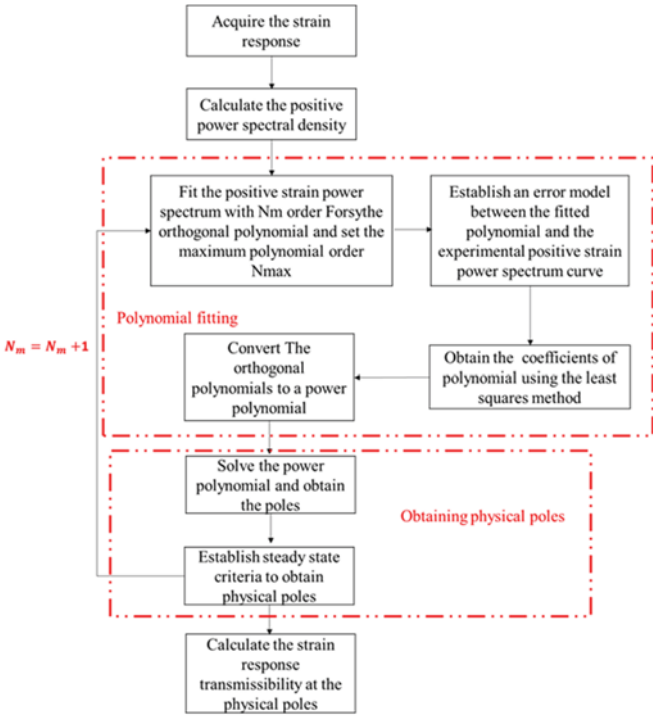

Figure 1. The diagram for the presented method for OMA

B. *The SDI for the bolt looseness detection*

When the bolt is loose, the natural frequency and SMS of the thin plate will change simultaneously. Herein, the procedure to construct a hybrid SDI combining the differences of natural frequency and SMS is presented as follows:

The difference in SMS is defined as follows:

$$\psi_{\Delta r}^{\varepsilon}(i) = |\psi_{dr}^{\varepsilon}(i) - \psi_{hr}^{\varepsilon}(i)| \tag{9}$$

where $\psi_{dr}^{\varepsilon}(i)$ denotes the r[th] strain mode shape concerning the i[th] element under the damaged structure. $\psi_{hr}^{\varepsilon}(i)$ denotes the r[th] strain mode shape about the i[th] element under the healthy structure. The difference of the modal strain is normalized as follows:

$$\psi_{\mathrm{N},\Delta\ r}^{\varepsilon}(i) = \frac{\psi_{\Delta r}^{\varepsilon}(i)}{\underbrace{max[\psi_{\Delta r}^{\varepsilon}(i)]}_{i}} \tag{10}$$

The average normalized mode strain differences of the first M order of the structure can be calculated by the following formula:

$$Average(\psi_{\mathrm{N},\Delta r}^{\varepsilon}(i)\ ) = \frac{1}{M}\sum_{r=1}^{M}\psi_{\mathrm{N},\Delta r}^{\varepsilon}(i) \tag{11}$$

The natural frequency change rate of the structure before and after the bolt loosening can be calculated by the following equation:

$$\omega_{r,\Delta} = \frac{|\omega_{r,d} - \omega_{r,h}|}{\omega_{r,h}} \tag{12}$$

Then the hybrid SDI can be obtained in (13), which is different from the SDI presented in [12].

$$Average(\omega_{r,\Delta}\cdot\psi_{\mathrm{N},\Delta r}^{\varepsilon}(i)) = \frac{1}{M}\sum_{r=1}^{M}\omega_{r,\Delta}\cdot\psi_{\mathrm{N},\Delta r}^{\varepsilon}(i) \tag{13}$$

With this operation, the differences of damage indicator will be amplified for the bigger change of natural frequencies. What's more, for the sake of excluding the impact of the unknown excitation, (13) has been widely used to calculate the modal strain transmissibility. $\boldsymbol{\psi}_r^{\varepsilon}$ is a normalized result with a maximum value of 1. The average rate of change of the first M order modal strain differences of the structure is calculated by (10) and (11). Therefore, the structural damage unit can be defined as follows:

$$Damaged\ elemnts = \{i: |Average(\omega_{r,\Delta}\cdot\psi_{\mathrm{N},\Delta r}^{\varepsilon}(i)) > \sigma\} \tag{14}$$

In the equation, σ denotes the threshold which can be determined statistically. Specific means of obtaining threshold can be found in [13]. The average process reduces the influence of uncertainty and noise.

III. THE SCENARIOS OF THE SIMULATIONS AND EXPERIMENTS

For illustrative purposes, the simulation and experiment were utilized to verify the proposed method for detecting the bolts looseness. The cantilever thin plate structure connected with the support base by 6 screws (M8) will be employed. The length of the cantilever plate is 400 mm, the width of the plate is 180 mm and its thickness is 5 mm. The material properties of the plate, supports and bolts were shown in Table I. The boundary conditions of the ANSYS model are given as follows: the bottom of the support is fixed constraint, the bolt and the support are set as binding constraint and the bolt and the thin plate are set as non-separating constraint. The meshing of the cantilever plate and numbering of the bolts are shown in Fig. 2 (a). The test system consisted of several FBG sensors, a dynamic FBG demodulator with a sampling frequency of 2 kHz, a hammer and a computer are shown in Fig. 2 (b) and 2 (c). When the 6 bolts were well connected, the pre-tightening torque of each bolt is 9 Nm to define the healthy condition. The experimental excitation is applied at different positions on the surface of the entire sheet.

Four tested conditions, i.e. Health: all bolts were well connected; Case 1: the bolts of $1^{\#}$ and $2^{\#}$ were loose, the remaining bolts were well connected; Case 2: the bolts of $1^{\#}$, $2^{\#}$ and $3^{\#}$ were loose, the remaining bolts were well connected; Case 3: the bolts of $1^{\#}$, $2^{\#}$, $3^{\#}$ and $4^{\#}$ were loose, the remaining two bolts were well connected are deigned.

TABLE I. PARAMETERS OF THE EXPERIMENTAL DEVICE

	The plate	Bearings and bolts
Material	7075 aluminum alloy	steel
Elastic modulus	71 Gpa	200 Gpa
Poisson ratio	0.33	0.3
Density	2810 kg/m^3	7850 kg/m^3

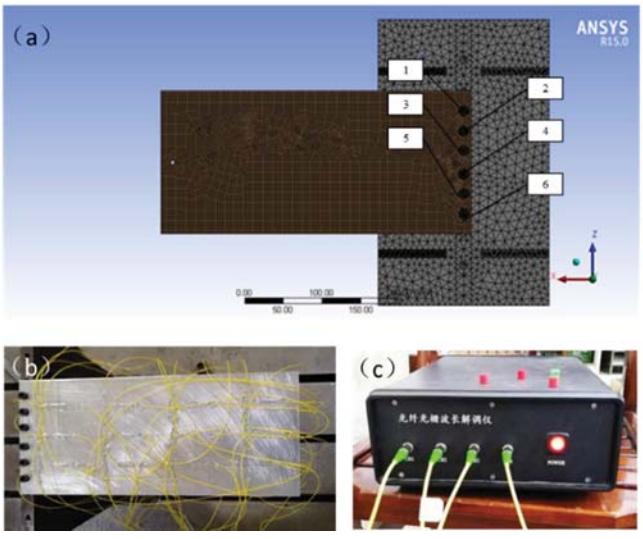

Figure 2. Schematic diagram of simulation and experimental equipment

IV. RESULTS AND DISCUSSION

A. Results from the finite element model (FEM)

The ANSYS WORKBENCH is used to analyze the plate under different tested cases. The calculated first six natural frequencies of the plate from ANSYS WORKBENCH under different cases are shown in Table II.

TABLE II. THE FIRST SIX NATURAL FREQUENCIES UNDER FOUR TESTED CONDITIONS

	Health	Case 1	Case 2	Case 3
1th natural frequency(Hz)	28.415	27.461	26.138	24.201
2th natural frequency(Hz)	126.47	119.29	110.66	97.932
3th natural frequency(Hz)	176.77	170.89	164.74	157.66
4th natural frequency(Hz)	408.51	348.52	292.95	231.94
5th natural frequency(Hz)	430.07	380.92	336.72	281.82
6th natural frequency(Hz)	493.57	476.29	459.61	442.89

From Table Π, the lowest six natural frequencies decrease with the increase of the loose degrees. However, the natural frequency as a physical quantity representing the overall characteristics of the structure cannot locate the loose bolts. Note that the torsional modes are not considered here. Only the 1st and 3rd bending SMSs are considered and shown in Fig. 3 and Fig. 4 respectively.

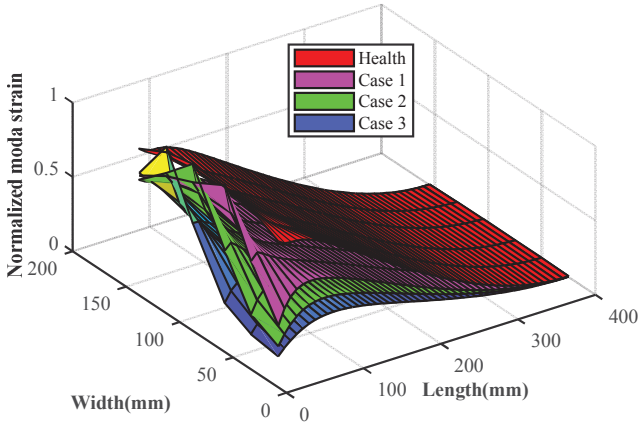

Figure 3. The first-order SMS of plate-simulation

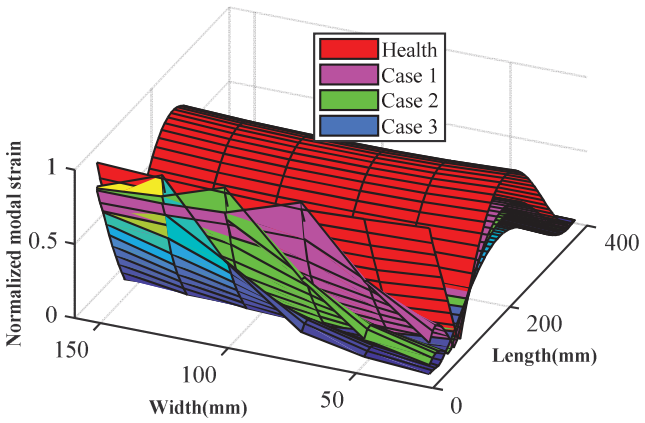

Figure 4. The third-order SMS of plate-simulation

As shown in Fig. 3 and Fig. 4, the differences of SMS for the plate near the loose bolts increased as the number of loose bolts increases. In order to validate that the presented SDI can be used to locate the loose bolts, the following threshold in (15) is considered.

$$\sigma = \frac{1}{n_o}\sum_{i=1}^{n_o}\left(\frac{1}{M}\sum_{r=1}^{M}\omega_{r,\Delta}\cdot\psi^{\varepsilon}_{\mathrm{N},\Delta r}(i)\right) + \chi\cdot\sqrt{\frac{1}{n_o-1}\cdot\sum_{i=1}^{n_o}\left(\frac{1}{M}\sum_{r=1}^{M}\omega_{r,\Delta}\cdot\psi^{\varepsilon}_{\mathrm{N},\Delta r}(i)-\frac{1}{n_o}\sum_{i=1}^{n_o}\left(\frac{1}{M}\sum_{r=1}^{M}\omega_{r,\Delta}\cdot\psi^{\varepsilon}_{\mathrm{N},\Delta r}(i)\right)\right)} \quad (15)$$

where n_0 represents the degree of freedom of the tested structure, χ represents the safety factor. In practical application, the safety factor should be determined by statistical methods or professional knowledge. Herein, we choose χ = -0.1 to verify the proposed method. The calculated SDI value and its threshold were shown in Fig. 4. Note that the measured points are selected near the bolts, for example, the point 1 is near the bolt 1 which is numbered in Fig. 2 (a).

As illustrated in Fig. 5, the loose bolts can be detected and located based on the presented SDI. What's more, the SDI increases with respect to the increase of the looseness degrees. Therefore, the SDI can quantify the relative looseness degrees of the bolts.

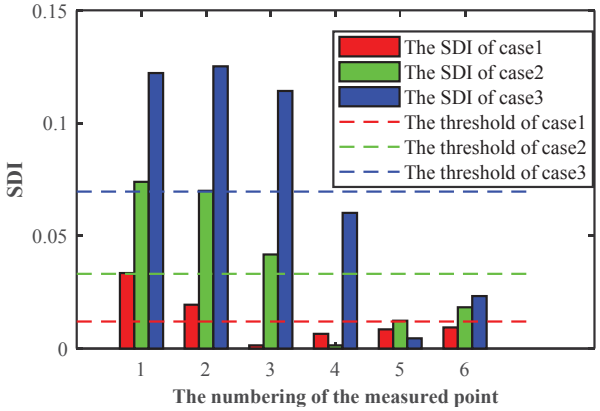

Figure 5. The SDI under different tested conditions-simulation

B. *Results from the experiments*

The stabilization diagram under the four tested conditions was displayed in Fig. 6. From Fig. 6, the natural frequencies are identified and listed in Table. III. And then the 1st order and 3rd order normalized modal strain for the all tested cases are further displayed in Fig. 7 and Fig. 8 respectively.

TABLE III. THE 1ST AND 3RD NATURAL FREQUENCIES UNDER FOUR OPERATING CONDITIONS

	Health	**Case 1**	**Case 2**	**Case 3**
1 th natural frequency(Hz)	26.65	25.5	23.91	18.34
3 th natural frequency(Hz)	165.5	158.6	152.2	137.2

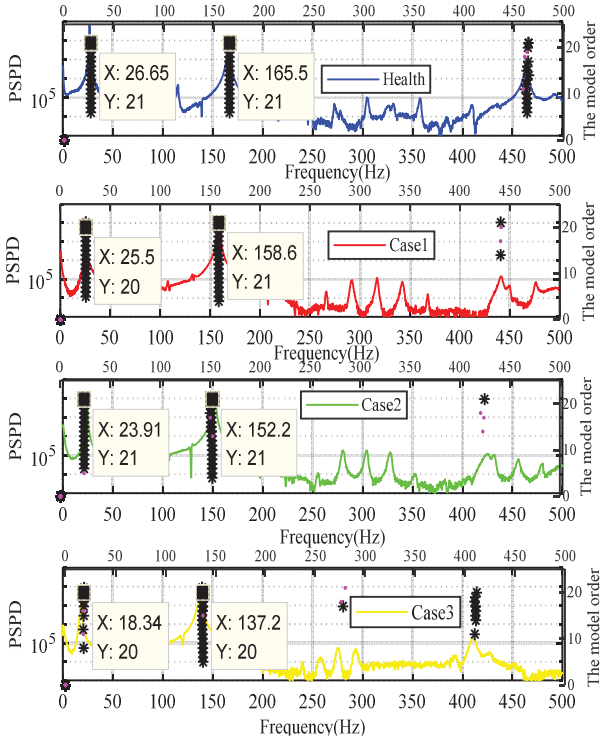

Figure 6. The stabilization diagram

From Fig. 7 and 8, it is so clear that the differences of the normalized modal strain in the loose positions between the healthy and the loose increase with the increase of the looseness degrees. The calculated SDIs for the tested cases are further shown in Fig. 9.

Note that the 1st FBG is responsible for detecting the looseness of the 1# and 2# bolts, the 2nd FBG is responsible for detecting the looseness of the 3# and 4# bolts and the 3rd FBG is responsible for detecting the looseness of the 5# and 6# bolts. As can be seen from Fig. 9, the looseness of the 1# and 2# bolts can be detected under case 1 based on the SDI. The 1# and 2# bolts must be loose, although, 3# and 4# bolts cannot determine whether both of them are loose under the case 2, we can locate the loose regions. The same conclusion can be drawn for the case 3.

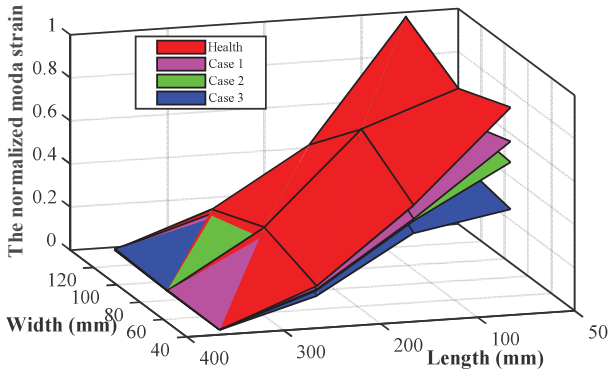

Figure 7. The 1st order modal strain modes of experiment

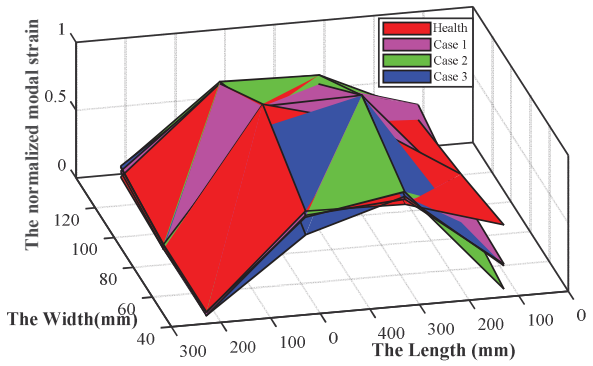

Figure 8. The 3rd order modal strain modes of experiment

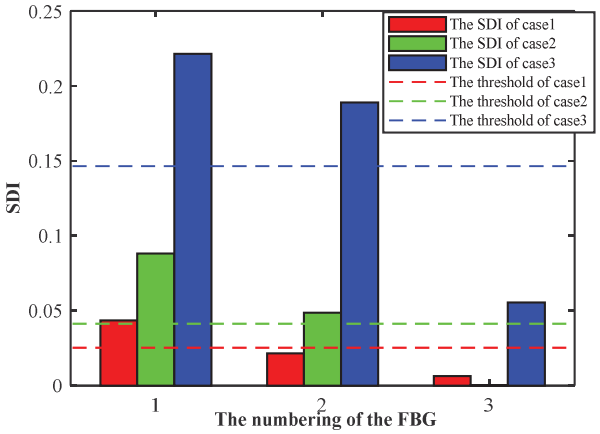

Figure 9. The histogram of SDI under different conditions of experiment

V. CONCLUSIONS

A method to detect the bolts looseness is presented in this work based on the operational modal strain identified from the FBG based OSMA. Specifically, an improved method of the OMA presented in our previous work is employed. And then an enhanced Structural Damage Indicator (SDI) based on the operational strain is presented to detect and locate the loose bolts. Both the results from simulations and experiments showed that the SDI can accurately detect and locate the loose bolts. Note that the looseness will deteriorate from the weakness of the structure, i.e. the loosened bolts. Therefore, we just consider the adjacent bolts in this work. In the future work, we will consider the non-adjacent bolts to further validate the capability of the presented method to detect the looseness of the non-adjacent bolts.

ACKNOWLEDGMENT

This work was supported by the Natural Science Foundation of China(No.51505353).

REFERENCES

[1] Li Li, Hao Zhi, Tongjin Li, Hairong Yu, and Kuicheng Gong, “Numerical calculation of flexible plate in flexible wall nozzle of wind tunnel,” The 2nd China CAE Analysis Technology Annual Conference, 2006.

[2] Wenzhong Qu, Mengyang Zhang, Junyu Zhou and Li Xiao, “Using sub-harmonic resonance to detect bolted joint looseness,” Journal of Vibration, Measurement & Diagnosis, vol. 37, pp. 279–283, April 2017.

[3] M Zhang, Y Shen, L Xiao, et al, “Application of sub-harmonic resonance for the detection of bolted joint looseness,” Nonlinear dynamics, vol. 88, pp. 1-11, 2017.

[4] Baiyong Gou, Qiuhai Lu, Bo Wang and Shiying Wang, “Bolt tightening force detection using outlier analysis of structural natural frequencies,” Journal of Vibration and Shock, vol. 34, pp. 77–82, 2015.

[5] Kyung-Young Jhang, Hai-Hua Quan, Job Ha, Noh-Yu Kim, “Estimation of clamping force in high-tension bolts through ultrasonic velocity measurement,” Ultrasonics, vol. 44, pp. 1339–1342, 2006.

[6] Yam, L.Y., Leung, T.P., Li, D.B. and Xue, K.Z., “The oretical and experimental study of modal strain analysis,” Journal of Sound and Vibration, vol. 191, pp. 251–260, March 1996.

[7] Desheng Jiang, Pei Luo and Lei Liang, “Fiber bragg grating sensor and recognition of structuraldamage based on strain modal theory,” Instrument Technique and Sensor, pp. 17–19, 2003.

[8] Yanwei Xu and Yuegang Tan, “Stiffened plate bolts loose recognition based on strain mode,” Mechanical Engineering & Automation, pp. 166–170, April 2017.(in Chinese)

[9] Zechao Wang, Mingyao Liu, Zaisi Zhu, et al. “Clamp looseness detection using modal strain estimated from FBG based operational modal analysis,” Measurement,vol 137, pp. 82–97, April 2019.

[10] W Heylen, S Lames, and P Sas, “Modal analysis theory and testing,” K.U Leuven, Belgium, 1997.

[11] B, Petters. System identification and damage detection in civil engineering, PhD thesis, Unversity of Leuven, Belgium, 2000.

[12] H.Y Cui, X Xu, W.Q Peng, Z.H Zhou, M Hong. “A damage detection method based on strain modes for structures under ambient excitation,” Measurement, vol 125, pp. 438-446, 2018.

[13] Y.H, An; B.F, Spencer, J.P, Ou, “A test method for damage diagnosis of suspension bridge suspender cables,” Computer-Aided Civil and Infrastructure Engineering, vol 30, pp. 771–784, 201